JOURNAL OF GEOPHYSICAL RESEARCH, VOL. 114, D00D11, doi:10.1029/2008JD011372, 2009

Click Here for Full Article

How well do IPCC-AR4/CMIP3 climate models simulate global dimming/brightening and twentieth-century daytime and nighttime warming?

Martin Wild[1]

Received 29 October 2008; revised 12 January 2009; accepted 28 January 2009; published 1 May 2009.

[1] Observations indicate that greenhouse induced twentieth-century warming has been strongly modulated by variations in surface solar radiation. Between the 1950s and 1980s, declining surface solar radiation (“global dimming”) likely caused a dampening of global warming, whereas increasing surface solar radiation (“brightening”) may have contributed to the rapid warming in the last 2 decades, and possibly also in the first half of the twentieth century. This is also reflected in the decadal evolution of diurnal temperature range, which is highly correlated with surface solar radiation, and which shows a distinct transition from a strong decrease between the 1950s and 1980s, toward a leveling off thereafter. The present study investigates to what extent these effects are simulated in the latest generation of global climate models used in the fourth Intergovernmental Panel on Climate Change (IPCC) assessment report (AR4) (phase 3 of the Coupled Model Intercomparison Project (CMIP3) models). While these models reproduce the overall twentieth century warming over global land surfaces well, they underestimate the decadal variations in the warming and particularly also in diurnal temperature range, indicative of a lack of decadal variations in surface solar radiation in the models.

Citation: Wild, M. (2009), How well do IPCC-AR4/CMIP3 climate models simulate global dimming/brightening and twentieth-century daytime and nighttime warming?, *J. Geophys. Res.*, *114*, D00D11, doi:10.1029/2008JD011372.

1. Introduction

[2] Global warming is considered as a major threat for life on our planet. Observations show that global mean temperature at the earth’s surface has substantially increased over the twentieth century [*Intergovernmental Panel on Climate Change*, 2007]. This increase, however, has not been linear over the past decades, but showed a much stronger warming from the 1980s to 2000 than from the 1950s to the 1980s. *Wild et al.* [2007] attributed the lack of significant warming from the 1950s to the 1980s to the decline in surface solar radiation observed over this period (“global dimming” [*Stanhill and Cohen*, 2001; *Gilgen et al.*, 1998; *Liepert*, 2002]), which may have effectively masked the greenhouse induced warming. Since the mid-1980s, however, the majority of the observation sites did not show a decrease in surface solar radiation anymore, or even pointed toward an increase (“brightening”) [*Wild et al.*, 2005; *Pinker et al.*, 2005]. *Wild et al.* [2007] suggested that the absence of surface solar dimming and associated masking effects since the 1980s allowed the greenhouse induced warming to become more evident, resulting in a more rapid temperature increase than in previous decades.

[1]Institute for Atmospheric and Climate Science, ETH Zurich, Zurich, Switzerland.

0148-0227/09/2008JD011372$09.00

[3] Global climate models (GCMs) are the most powerful tools currently available to investigate climate change issues. In the present study I explore to what extent the current generation of GCMs used in the Intergovernmental Panel on Climate Change (IPCC) fourth assessment report (IPCC-AR4) [*IPCC*, 2007] is capable of reproducing this characteristic behavior in temperature evolution over the past decades. The focus thereby is not only on mean temperatures, but also on daily maximum and minimum temperatures and related diurnal temperature range (DTR), which allow a better separation of the solar and terrestrial radiative effects on temperature [*Wild et al.*, 2007; *Makowski et al.*, 2008].

2. Models and Observational Data

[4] For the present study I analyzed data from the latest generation of GCMs participating in the experiments for IPCC-AR4 [*IPCC*, 2007]. These model data have been organized by the Program for Climate Model Diagnosis and Intercomparison (PCMDI). I focused on the “20th Century Climate in Coupled Models (20C3M)” experiments therein. These experiments were aimed at reproducing the climate evolution of the twentieth century as accurately as possible, by considering the major natural and anthropogenic forcings, such as changes in atmospheric greenhouse gases, aerosol load (tropospheric and volcanic), solar output, and land use. These experiments are therefore best suited for the assessment of the capability of the models to reproduce the climate evolution over the past decades. A more detailed description of the forcings used in these experiments is

Table 1. List of IPCC-AR4/CMIP3 Climate Models Analyzed in the Present Study, With Their Abbreviations and Associated Research Organizations[a]

Model Abbreviation	Research Organization
cccma_cgcm3_1/cgcm3_1_t63	Canadian Centre for Climate Modeling and Analysis (CCCMA), Canada
cnrm_cm3	Centre National de Recherches Meteorologiques (CNRM), France
csiro_mk3_0/mk3_5	Commonwealth Scientific and Industrial Research Organisation (CSIRO), Australia
gfdl_cm2_0/cm2_1	Geophysical Fluid Dynamics Laboratory (GFDL), New Jersey
giss_ model_e_r/e_h/aom	Goddard Institute for Space Studies (GISS), New York
iap_fgoals1_0_g	Institute of Atmospheric Physics (IAP), Beijing, China
inmcm3_0	Institute for Numerical Mathematics (INM), Moscow, Russia
ipsl_cm4	Institut Pierre Simon Laplace (IPSL), France
miroc3_2_medres/hires	Center for Climate System Research (CCSR), Japan
miub_echo_g	Meteorological Institute of the University of Bonn (MIUB), Germany
mpi_echam5	Max-Planck-Institut for Meteorology (MPI), Germany
ncar_ccsm3_0/pcm1	National Center for Atmospheric Research (NCAR), Colorado

[a]For more information on individual models, the reader is referred to the Web pages of the Program for Climate Model Diagnosis and Intercomparison (PCMDI) (http://www-pcmdi.llnl.gov/) and links therein as well as to *IPCC* [2007, chapter 8].

provided on the web pages of the PCMDI (http://www-pcmdi.llnl.gov/). These experiments form a part of the phase 3 of the Coupled Model Intercomparison Project (CMIP3).

[5] For the present study most relevant are the forcings related to aerosol direct and indirect effects, which modify the simulated surface solar radiation. All models taking part in the IPCC-AR4/CMIP3 experiments consider to some extent changes in sulfate aerosol burden, but only three models include an explicit treatment of the sulfur cycle. Black carbon aerosols are only considered by a minority of the models. This applies also to the indirect aerosol effects (aerosol induced changes in cloud optical properties as well as cloud lifetime), which are not implemented in the majority of the models (see also *IPCC* [2007, Table 10.1] for details of the individual models).

[6] Surface temperature and radiation fields are available from 18 models participating in the 20C3M experiments (see Table 1 for model abbreviations and associated research organizations). Eight of these models also store daily maximum and minimum temperatures and therefore the diurnal temperature range, which is another focus of this study. These eight models are from NCAR (model versions ccsm3 and pcm1), GISS (model version aom), CCSR (model versions miroc3_2 medium and high resolution), CSIRO (model versions mk3_0 and mk3_5) and INM (model version cm3). Except the CCSR models, none of these eight models include the indirect aerosol effects. Also, the majority of these models include only sulfate aerosols, except for the CCSR models and NCAR ccsm3, which include in addition black and organic carbon aerosols.

[7] Observations on the evolution of mean as well as daily maximum and minimum temperatures are taken from the gridded data set provided by the Climate Research Unit (CRU), University of East Anglia [*Mitchell and Jones*, 2005]. This data set provides observed daily mean, maximum and minimum temperatures as monthly averages over the period 1900–2002 on a 0.5° grid. Annual values of global and hemispheric temperature estimates are approximately accurate to ±0.05°C (2 standard errors) for the period since 1951 [*Brohan et al.*, 2006].

3. Results

[8] As in the study by *Wild et al.* [2007] I focus on the period starting from the International Geophysical Year (IGY) 1958, when widespread measurements of surface radiation were initiated, up to 1999, when the 20C3M experiments end. We thereby focus on land surfaces, where we have the best information on the variations in the temperature indices and surface solar radiation. In the following, we subdivide the analysis into two periods, 1958–1985 and 1985–1999. The former covers a period, when radiation observations indicate a dominance of surface solar dimming, while in the latter period, rather a tendency toward a brightening is observed [*Wild et al.*, 2005].

3.1. Decadal Changes in Mean 2-m Temperature

[9] During the period 1958–1985, the observed annual mean temperature over terrestrial surfaces has only slightly increased, by 0.04°C/decade [*Wild et al.*, 2007]. The related mean surface temperature fields were available from 18 IPCC-AR4/CMIP3 models. With a mean and median increase of 0.14°C/decade and 0.17°C/decade, respectively, the models simulate in general a substantially stronger increase over this period than indicated by the observations (Figure 1 and Table 2). Specifically, 13 out of the 18 models simulate a stronger increase than observed.

[10] On the other hand, during the period 1985–1999, the models simulate a smaller temperature increase over terrestrial surfaces than observed. The observed increase over this period is as much as 0.38°C/decade, while the mean and median increases in the 18 models are 0.23°C/decade and 0.22°C/decade, respectively (Figure 1 and Table 2). Out of the 18 models, 15 models show a less pronounced increase than observed, while only three models exceed the observed warming. This gives a first indication, that neither the damping effect of declining surface solar radiation nor the enhancing effect of more recent surface solar brightening has been taken into account to its full extent by the models. Note that over the entire period under consideration here, 1958–1999, the multimodel mean is, at 0.18°C/decade, close to the observed increase of 0.17°C/decade over the same 1958–1999 period. This suggests that the models do reproduce the longer-term trends well, in line with the findings of *IPCC* [2007]. Yet, it is the result of a compensation between an overestimated warming during the first part of the period under consideration, and an underestimation thereafter. This indicates that the current generation of GCMs is able to reproduce observed temperature trends on multidecadal to centennial timescales, but underestimates decadal-scale variations.

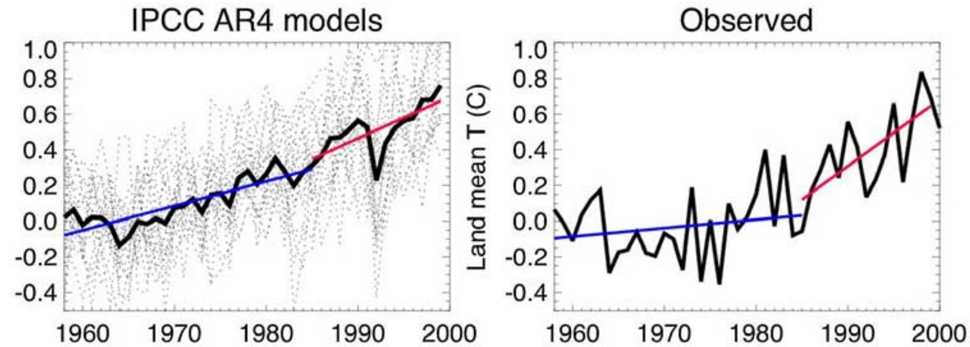

Figure 1. Annual mean temperature anomalies over global land surfaces from 1958 to 1999, as (left) simulated by 18 GCMs in twentieth-century experiments performed for the fourth IPCC assessment report and (right) observed. Multimodel mean is given as thick black line, and individual model realizations are shown as dashed lines. Linear regressions for the periods 1958–1985 are in blue and for 1985–1999 are in red. Observations from the CRU data set [*Mitchell and Jones*, 2005]. Reference period for anomalies is the entire twentieth century. Unit is °C.

This may hamper the predictive skills of these models to project near future climate evolution.

3.2. Decadal Changes in Daily Maximum and Minimum Temperatures

[11] In addition to the analysis of mean temperature, the analysis of the daily maximum and minimum temperatures holds the potential to disentangle the influence of surface solar and thermal radiation on global warming. This is due to the fact that solar and thermal radiation have different effects on these diurnal temperature extremes. Since the solar flux is obviously only present during daylight, it affects the daily maximum temperature (TMAX) more than daily minimum temperature (TMIN). The nighttime minimum temperature, on the other hand, is mainly affected by the thermal radiative exchanges. Nighttime surface radiative cooling depends on the capacity of the atmosphere to absorb and reemit thermal radiation toward the surface. An analysis of TMIN and TMAX therefore allows a cleaner separation of solar and thermal radiation influences on surface temperature than an analysis of the mean temperature alone. *Wild et al.* [2007] noted distinctly different changes in the observed TMAX and TMIN during the period 1958–1985, with TMAX slightly decreasing, while TMIN increased. *Wild et al.* [2007] related the decrease in TMAX to the decrease in surface solar radiation prevailing over this period. In contrast, in the more recent period 1985–1999, observed TMAX and TMIN both increased at similar rates, in line with the absence of surface solar dimming to suppress daytime warming in this period [*Wild et al.*, 2007].

Table 2. Linear Changes in Annual Mean 2-m Temperature Over Global Land Surfaces for the "Dimming" Period 1958–1985, the "Brightening" Period 1985–1999, and the Difference Between the Changes in the Latter and Former Periods, as Simulated by 18 GCMs Participating in the Fourth IPCC Assessment Report and as Observed[a]

Model	1958–1985	1985–1999	Difference
cccma_cgcm3_1	0.40 (0.03)	0.20 (0.06)	−0.20
cccma_cgcm3_1_t63	0.30 (0.03)	0.43 (0.11)	0.13
cnrm_cm3	0.24 (0.06)	0.13 (0.15)	−0.11
csiro_mk3_0	0.19 (0.03)	0.04 (0.12)	−0.15
csiro_mk3_5	0.18 (0.06)	0.26 (0.13)	0.08
gfdl_cm2_0	−0.05 (0.04)	0.58 (0.14)	0.63
gfdl_cm2_1	−0.01 (0.07)	0.57 (0.22)	0.58
giss_aom	0.11 (0.03)	0.16 (0.07)	0.05
giss_model_e_h	0.03 (0.04)	0.12 (0.11)	0.09
giss_model_e_r	0.01 (0.04)	0.23 (0.15)	0.22
iap_fgoals1_0_g	0.17 (0.05)	0.12 (0.15)	−0.05
inmcm3_0	0.20 (0.04)	0.13 (0.15)	−0.07
ipsl_cm4	0.12 (0.04)	0.23 (0.07)	0.11
miroc3_2_hires	0.13 (0.04)	0.34 (0.09)	0.21
miroc3_2_medres	0.06 (0.05)	0.09 (0.10)	0.03
miub_echo_g	0.01 (0.05)	0.28 (0.17)	0.27
mpi_echam5	0.18 (0.07)	0.23 (0.10)	0.05
ncar_ccsm3_0	0.21 (0.04)	0.06 (0.16)	−0.15
Mean model change	0.14	0.23	0.09
Median model change	0.17	0.22	0.05
Observed change	0.04 (0.04)	0.38 (0.08)	0.34

[a]Observed changes are determined from the CRU data set [*Mitchell and Jones*, 2005]. One-sigma uncertainties are given in parentheses. Also shown are the multimodel mean and median changes. Units are °C/decade.

[12] Eight of the models participating in IPCC-AR4/CMI3 provide TMAX and TMIN fields and allow an assessment of these quantities (see section 2). Over the period 1958–1985, none of the models reproduces the decrease in TMAX as indicated in the observations. Instead, all models show an increase over this period, which is above the 1-sigma uncertainty level in seven out of eight models (Figure 2, top, and Table 3). The models simulate a mean and median linear increase in TMAX of 0.13°C/decade and 0.16°C/decade, respectively, while the observations suggest a decrease of −0.04°C/decade.

[13] On the other hand, none of the models reproduces the strong observed increase in TMAX in the more recent period (Figure 2, top, and Table 3). The simulated mean and median increase between 1985 and 1999 amounts to 0.14°C/decade and 0.15°C/decade, respectively, while the observed increase is with 0.39°C/decade substantially larger. The observed increase in TMAX lies outside the range of model increases even when the 1-sigma uncertainty estimates given in Table 3 are added.

[14] The change in the regression slope of TMAX between the two periods thus amounts to +0.43 in the observations, but only to +0.01 and −0.01 in the multimodel mean and median, respectively (Table 3). Since TMAX is strongly affected by insolation, this gives further indication that the

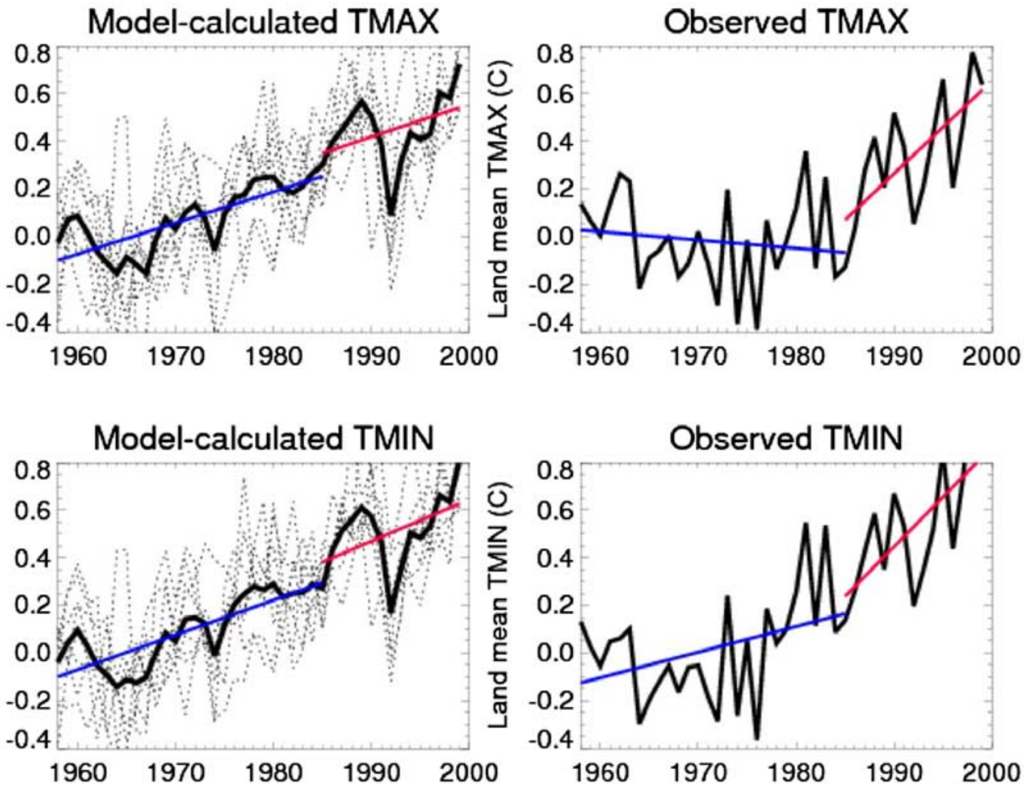

Figure 2. Annually averaged daily (top) maximum temperature and (bottom) minimum temperature anomalies over global land surfaces from 1958 to 1999, as (left) simulated by eight GCMs in twentieth-century experiments performed for the fourth IPCC assessment report and (right) observed. Multimodel mean is given as thick black line, and individual model realizations are shown as dashed lines. Linear regressions for the periods 1958–1985 are in blue and for 1985–1999 are in red. Observations from the CRU data set [*Mitchell and Jones*, 2005]. Reference period for anomalies is the entire twentieth century. Unit is °C.

models may not properly take into account the suppression of changes in TMAX by declining insolation during the dimming period, nor the acceleration of the TMAX changes during the brightening period.

Table 3. Linear Changes in TMAX Over Global Land Surfaces for the "Dimming" Period 1958–1985, the "Brightening" Period 1985–1999, and the Difference Between the Changes in the Latter and Former Periods, as Simulated by the Eight GCMs Participating in the Fourth IPCC Assessment Report Which Provided TMAX Data and as Observed[a]

Model	1958–1985	1985–1999	Difference
inmcm3_0	0.20 (0.04)	0.15 (0.15)	−0.05
csiro_mk3_0	0.16 (0.04)	−0.01 (0.13)	−0.17
csiro_mk3_5	0.18 (0.07)	0.24 (0.13)	0.06
miroc3_2_hires	0.16 (0.04)	0.24 (0.10)	0.08
miroc3_2_medres	0.04 (0.06)	0.05 (0.11)	0.01
giss_aom	0.10 (0.03)	0.17 (0.07)	0.07
ncar_ccsm3_0	0.07 (0.05)	0.11 (0.14)	0.04
ncar_pcm1	0.14 (0.04)	0.14 (0.16)	0.00
Mean model change	0.13	0.14	0.01
Median model change	0.16	0.15	−0.01
Observed change	−0.04 (0.04)	0.39 (0.08)	0.43

[a]TMAX denotes daily maxima temperatures. Observed changes are derived from the CRU data set [*Mitchell and Jones*, 2005]. One-sigma uncertainties are given in parentheses. Also shown are the multimodel mean and median changes. Units are °C/decade.

[15] In the TMIN evolution, less directly affected by surface solar radiation, the discrepancies between observed and modeled tendencies are less pronounced, particularly in the first period 1958–1985. During this period, the model-calculated mean and median increase is 0.15°C/decade and 0.17°C/decade, respectively, while observations show an increase of 0.11°C/decade (Figure 2, bottom, and Table 4). The remaining overestimation in the TMIN increase might be explained by the fact that the excessive daytime warming can exert some influence also on nighttime warming through the inertia inherent in the Earth surface and atmospheric boundary layer. It is also noteworthy, that the models, on average, show a very similar increase in TMIN and in TMAX during the "dimming" period 1958–1985, with TMAX increasing by 0.13°C/decade, and TMIN by 0.15°C/decade (Tables 3 and 4 and Figure 2). This is in contrast to the observations which show a decrease in TMAX of −0.04°C/decade, but an increase in TMIN of 0.11°C/decade. Over the "brightening" period 1985–1999, model calculated changes in TMIN and TMAX are very similar, as is found in the observations. In absolute terms, however, both model-calculated TMIN and TMAX increases are less than 40% of the observed change over the 1985–1999 period.

3.3. Decadal Changes in Diurnal Temperature Range

[16] The Diurnal Temperature Range (DTR) is defined as the difference between TMAX and TMIN. This quantity is

Table 4. Linear Changes in TMIN Over Global Land Surfaces for the "Dimming" Period 1958–1985, the "Brightening" Period 1985–1999, and the Difference Between the Changes in the Latter and Former Periods, as Simulated by the Eight GCMs Participating in the Fourth IPCC Assessment Report Which Provided TMIN Data and as Observed[a]

Model	1958–1985	1985–1999	Difference
inmcm3_0	0.19 (0.05)	0.09 (0.16)	−0.10
csiro_mk3_0	0.21 (0.03)	0.09 (0.10)	−0.12
csiro_mk3_5	0.19 (0.06)	0.27 (0.12)	0.08
miroc3_2_hires	0.13 (0.04)	0.37 (0.10)	0.24
miroc3_2_medres	0.07 (0.05)	0.13 (0.10)	0.06
giss_aom	0.12 (0.03)	0.15 (0.07)	0.03
ncar_ccsm3_0	0.09 (0.05)	0.17 (0.15)	0.08
ncar_pcm1	0.17 (0.05)	0.15 (0.13)	−0.02
Mean model change	0.15	0.18	0.03
Median model change	0.17	0.15	−0.02
Observed change	0.11 (0.04)	0.42 (0.08)	0.31

[a]TMIN denotes daily minima temperatures. Observed changes are derived from the CRU data set [*Mitchell and Jones*, 2005]. One-sigma uncertainties are given in parentheses. Also shown are the multimodel mean and median changes. Units are °C/decade.

expected to be a better proxy for surface solar radiation variations than TMAX, since, after subtraction of TMIN from TMAX, thermal effects are to a considerable extent eliminated from the records. This leaves the solar influences as a major forcing factor of DTR, particularly integrated over large areas as considered here, where advective influences are minimized [*Makowski et al.*, 2008]. Indeed, several studies showed a very high correlation of observed records of surface solar radiation and DTR [e.g., *Bristow and Campbell*, 1984; *Liu et al.*, 2004; *Makowski et al.*, 2009]. A decline in observed DTR over global terrestrial surfaces after 1950 was documented in a number of studies [e.g., *Karl et al.*, 1993; *Easterling et al.*, 1997; *Dai et al.*, 1999]. *Wild et al.* [2007] pointed out that this decline underwent a significant transition during the 1980s, with a leveling off in the more recent years, in accord with *Vose et al.* [2004]. *Wild et al.* [2007] further pointed to the concurrence of the leveling off in DTR with the transition in surface radiative forcing from dimming to brightening. Similar findings were obtained on more regional scales based on 305 sites in China [*Liu et al.*, 2004] and on 168 sites in Europe [*Makowski et al.*, 2009]. The simulated DTR can be inferred from the eight IPCC-AR4/CMIP3 models above, which provide TMAX and TMIN. In Figure 3, simulated and observed global mean land DTR over the past decades are compared. The strong decline seen in the observations over the period 1958–1985 is not reproduced by the models. The model mean and median decline are both only −0.02°C/decade, while the observed decline is −0.15°C/decade, i.e., 1 order of magnitude larger (Table 5). None of the eight models shows a reduction to the extent as observed, even when the 1-sigma uncertainty estimates are taken into account (Table 5 and Figure 3). The models with the strongest reduction in DTR reproduce, at −0.04°C/decade between 1958 and 1985, only 30% of the observed reduction (Table 5). A lack of declining DTR in GCMs was also noted in previous studies based on earlier GCMs [e.g., *Kukla et al.*, 1995; *Stone and Weaver*, 2002, 2003, and references therein]. The negligible change in the DTR in the models over the 1958–1985 period is a result of the very similar changes in TMIN and TMAX noted in section 3.2, while the opposing changes (even in sign) of observed TMAX and TMIN induce the substantial decline in observed DTR over the same period. Since large-scale DTR changes may be considered as a valuable first-order proxy for surface solar radiation changes (see references given above), this is again an indication that a large-scale decline in surface solar radiation may have caused the decline in observed DTR. The decline in surface solar radiation may not be considered to its full extent in the models (see section 3.4). Also, while the observations show a strong positive change in the slope of the linear regression from the 1958–1985 to the 1985–1999 period of 0.12°C/decade, the change in the slope in the models is even slightly negative, at −0.02°C/decade (Table 5). This further suggests that the significant change in the surface radiative forcing regimes observed between the

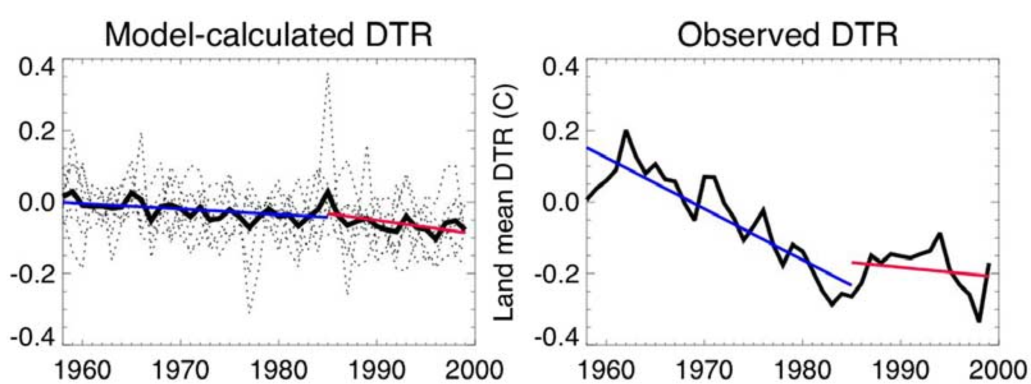

Figure 3. Annually averaged diurnal temperature range (DTR) anomalies over global land surfaces from 1958 to 1999, as (left) simulated by eight GCMs in twentieth-century experiments performed for the fourth IPCC assessment report and (right) observed. Multimodel mean is given as thick black line, and individual model realizations are shown as dashed lines. Linear regressions for the periods 1958–1985 are in blue and for 1985–1999 are in red. Observations from the CRU data set [*Mitchell and Jones*, 2005]. Reference period for anomalies is the entire twentieth century. Unit is °C.

Table 5. Linear Changes in DTR Over Global Land Surfaces for the "Dimming" Period 1958–1985, the "Brightening" Period 1985–1999, and the Difference Between the Changes in the Latter and Former Periods, as Simulated by the Eight GCMs Participating in the Fourth IPCC Assessment Report Which Provided DTR Data and as Observed[a]

Model	1958–1985	1985–1999	Difference
inmcm3_0	0.01 (0.03)	0.07 (0.07)	0.06
csiro_mk3_0	−0.04 (0.02)	−0.09 (0.05)	−0.05
csiro_mk3_5	−0.01 (0.02)	−0.03 (0.04)	−0.02
miroc3_2_hires	0.03 (0.02)	−0.12 (0.06)	−0.15
miroc3_2_medres	−0.03 (0.02)	−0.08 (0.03)	−0.05
giss_aom	−0.02 (0.01)	0.03 (0.02)	0.05
ncar_ccsm3_0	−0.02 (0.01)	−0.06 (0.03)	−0.04
ncar_pcm1	−0.04 (0.02)	−0.01 (0.04)	0.03
Mean model change	−0.02	−0.04	−0.02
Median model change	−0.02	−0.03	−0.01
Observed change	−0.15 (0.01)	−0.03 (0.02)	0.12

[a]DTR denotes diurnal temperature range. Observed changes are from the CRU data set [*Mitchell and Jones*, 2005]. One-sigma uncertainties are given in parentheses. Also shown are the multimodel mean and median changes. Units are °C/decade.

two periods ("from dimming to brightening") is not adequately reproduced in the models.

3.4. Decadal Changes in Surface Solar Radiation

[17] Since DTR was suggested as a valuable proxy for surface solar radiation in different studies as noted above, the above results may point to deficiencies in the GCM-simulated surface solar radiation. Specifically, this analysis showed that neither the strong observed decline in DTR between the 1960s and 1980s nor its transition to a leveling off in more recent years is reproduced in the models used in the IPCC-AR4. This points to a too weak decline in surface solar radiation ("dimming") in the model simulations between the 1960s and 1980s as well as their inability to capture the full extent of the transition from dimming to brightening in the mid-1980s. Therefore I also looked at the surface solar radiation simulated in the IPCC-AR4/CMIP3 models. Unlike DTR, TMAX and TMIN, which have only been available from eight of the models, the downwelling surface solar radiation has been again stored in all 18 models, as the mean temperature. Surface solar radiation simulated by these IPCC-AR4/CMIP3 models on a climatological mean basis has been evaluated in previous studies [*Wild et al.*, 2006; *Wild*, 2008]. They show that the models overall tend to overestimate surface solar radiation compared to a comprehensive set of surface measurements, under both all-sky and clear-sky conditions. Here the focus is instead on the decadal variation of the simulated fluxes. Figure 4 depicts the evolution of surface solar radiation over global land surfaces over the focal period 1958–1999 as calculated by the 18 models. Over the entire period the multimodel mean shows a slight decrease of −0.35 W m^{-2}/decade, which is nearly linear, except for the temporary reductions after major volcanic eruptions (Agung 1964, El Chichon 1983, Pinatubo 1991). The decrease is in line with *Romanou et al.* [2007], who found a global mean decrease of 1–4 W m^{-2} over the twentieth century in nine of these models. Over the period 1958–1985, a decrease of −0.43 W m^{-2}/decade is found in the multimodel mean over global land surfaces (Table 6). The decrease persists over the period 1985–1999, at −0.20 W m^{-2}/decade. Unlike temperature measurements, with their dense networks over terrestrial surfaces, the much fewer surface radiation sites make an unambiguous determination of observed global land mean estimates more difficult. The analyses of the available radiation measurements in the literature suggest declines of surface solar radiation from the 1960s to the 1980s, which are an order of magnitude larger than the changes simulated by the models in Table 6 for the 1958–1985 period [e.g., *Gilgen et al.*, 1998; *Stanhill and Cohen*, 2001, and references therein; *Liepert*, 2002; *Wild et al.*, 2004; *Wild*, 2009, and references therein]. Even though these estimates might be biased high to some extent owing to local pollution [*Alpert et al.*, 2005], the discrepancies between observational and model-calculated changes are considerable over this period. Satellite-derived estimates of surface solar radiation, which provide a global coverage [*Pinker et al.*, 2005; *Hatzianastassiou et al.*, 2005] are only available since the mid-1980s and thus cover only the second period (1985–1999) under consideration (see also N. Hatzianastassiou et al., Two-decadal trends of aerosol optical thickness and direct radiative effect on surface solar radiation and their role in global dimming and brightening, submitted to *Journal of Geophysical Research*, 2009). Satellite-derived estimates may be sensitive to uncertainties in some of their input data, such as changes in cloud and aerosol properties, which are difficult to infer from satellites. Accordingly, trends in satellite-derived estimates differ substantially [*Wild*, 2009]. Globally, the satellite-based estimates suggest a large-scale brightening since the mid-1980s, of +1.6 W m^{-2}/decade [*Pinker et al.*, 2005] or +3.5 W m^{-2}/decade (Hatzianastassiou et al., submitted manuscript, 2009) over periods closely matching the 1985–1999 period under consideration here. Over land surfaces only, estimates range from −0.5 W m^{-2}/decade [*Pinker et al.*, 2005] to +3.7 W m^{-2}/decade (Hatzianastassiou et al., submitted manuscript, 2009). *Wild et al.* [2008] derived an increase of +2.2 W m^{-2}/decade in solar radiation over global land surfaces over the same period

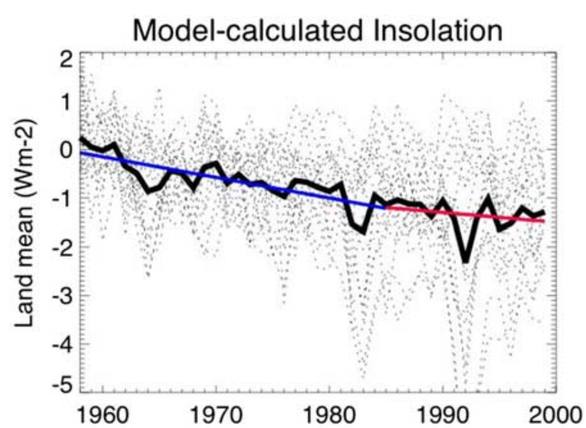

Figure 4. Annual averaged surface solar radiation anomalies over global land surfaces from 1958 to 1999, as simulated by 18 GCMs in twentieth-century experiments performed for the fourth IPCC assessment report. Multimodel mean is given as thick black line, and individual model realizations are shown as dashed lines. Linear regressions for the periods 1958–1985 are in blue and for 1985–1999 are in red. Reference period for anomalies is the entire twentieth century. Unit is W m^{-2}.

Table 6. Linear Changes in Annual Mean Downwelling Solar Radiation Over Global Land Surfaces for the "Dimming" Period 1958–1985, the "Brightening" Period 1985–1999, and the Difference Between the Changes in the Latter and Former Period, as Simulated by 18 GCMs Participating in the Fourth IPCC Assessment Report[a]

Model	1958–1985	1985–1999	Difference
cccma_cgcm3_1	0.04 (0.14)	0.19 (0.51)	0.15
cccma_cgcm3_1_t63	0.12 (0.16)	0.04 (0.32)	0.16
cnrm_cm3	0.34 (0.18)	0.15 (0.56)	0.19
csiro_mk3_0	0.41 (0.19)	0.41 (0.49)	0.00
csiro_mk3_5	0.04 (0.18)	0.24 (0.44)	0.20
gfdl_cm2_0	0.50 (0.18)	0.67 (0.65)	0.17
gfdl_cm2_1	0.56 (0.24)	0.47 (0.49)	0.09
giss_aom	0.29 (0.10)	0.33 (0.21)	0.62
giss_model_e_h	1.43 (0.22)	0.67 (0.69)	0.76
giss_model_e_r	1.11 (0.19)	0.32 (0.86)	0.79
iap_fgoals1_0_g	0.05 (0.13)	0.72 (0.36)	0.67
inmcm3_0	0.13 (0.10)	0.43 (0.34)	0.56
ipsl_cm4	0.30 (0.08)	0.11 (0.28)	0.41
miroc3_2_hires	0.66 (0.17)	0.13 (0.53)	0.79
miroc3_2_medres	0.68 (0.17)	0.51 (0.43)	0.17
miub_echo_g	0.46 (0.18)	0.19 (0.41)	0.27
mpi_echam5	0.42 (0.20)	0.55 (0.39)	0.97
ncar_ccsm3_0	0.38 (0.19)	0.64 (0.49)	0.26
Mean model change	0.43	0.20	0.23
Median model change	0.38	0.19	0.19

[a]One-sigma uncertainties are given in parentheses. Also shown are the multimodel mean and median changes. Units are W m^{-2}/decade.

on the basis of 332 surface radiation sites. Overall, the available literature does not support a continuation of the dimming over the 1985–1999 period as simulated in the GCMs [*Wild*, 2009]. The observational estimates, indicating an increasing surface solar radiation since the mid-1980s, are in line with evidence for decreasing background aerosol optical depths inferred from satellite measurements over the oceans during the 1990s [*Mishchenko et al.*, 2007] and a general decrease in anthropogenic sulfur and black carbon emissions during this period [*Stern*, 2006; *Streets et al.*, 2006]. For the area of Europe, *Ruckstuhl and Norris* [2009] find that a multimodel mean composed of 14 of the IPCC-AR4/CMIP3 models used here underestimates the decline in the clear sky surface solar radiation during the dimming period compared to the trends estimated from observations by *Ruckstuhl et al.* [2008] and *Norris and Wild* [2007]. They further note that the magnitude of the subsequent "brightening" under cloud free atmospheres over Europe is too small in the models compared to these references.

[18] Overall, compared to the evidence given in the literature on the evolution of surface solar radiation over the second part of the twentieth century, the GCMs seem to underestimate the decadal changes in this quantity. This is further illustrated in Figure 5. There the longest record with surface solar radiation observations available in GEBA, the Stockholm time series with more than 70 years of data back to 1923, is compared to the surface solar radiation as reproduced at the nearest grid point by the 18 IPCC-AR4/CMIP3 models in their 20C3M simulations. Figure 5 indicates that decadal variations of surface solar radiation simulated at the Stockholm grid point are much lower than observed. Note that in the multimodel mean, decadal variations can be artificially suppressed through the averaging process over the individual simulations. Yet, also an inspection of the individual model simulations shows that none of the models adequately captures the substantial decadal changes seen in the Stockholm time series. Specifically, the standard deviation of the observed annual mean time series lies, with 8.4 W m^{-2}, outside the range of variances simulated at the corresponding grid points by all 18 GCMs, which lie between 3.6 W m^{-2} to 8.1 W m^{-2}, with a mean value of 5.7 W m^{-2}.

[19] A more extended comparison of surface solar radiation with direct observations is planned for a future study.

4. Discussion and Conclusions

[20] Independent analyses of different temperature indices and surface solar radiation trends simulated in the "20th Century Climate in Coupled Models (20C3M)" experiments indicate that decadal dimming and brightening and related temperature effects are not reproduced to their full extent in current climate models. This may also explain why the simulated mean temperature increase over land surface is too strong in the "dimming phase" and too weak in the "brightening phase" (Figure 1 and Table 2).

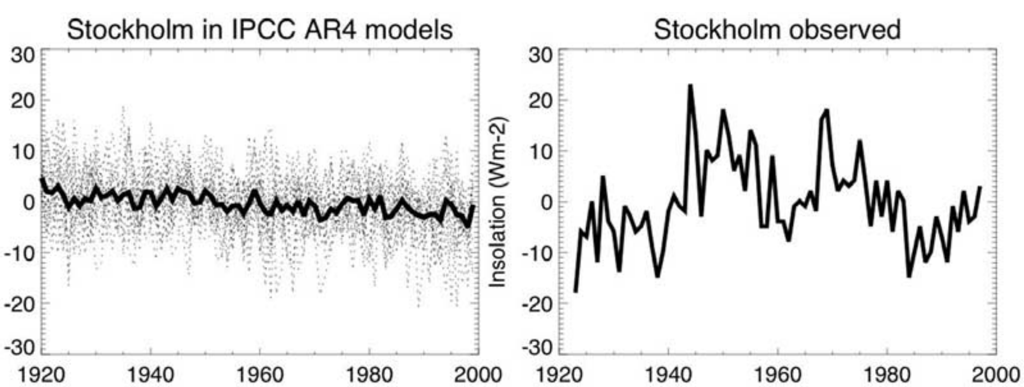

Figure 5. Annual mean surface solar irradiance anomalies as (right) observed at the long-term monitoring station Stockholm and (left) simulated at the respective grid point by 18 GCMs in twentieth-century experiments performed for the fourth IPCC assessment report. Multimodel mean is given as thick black line, and individual model realizations are shown as dashed lines. Reference period for anomalies is 1923–1999. Unit is W m^{-2}.

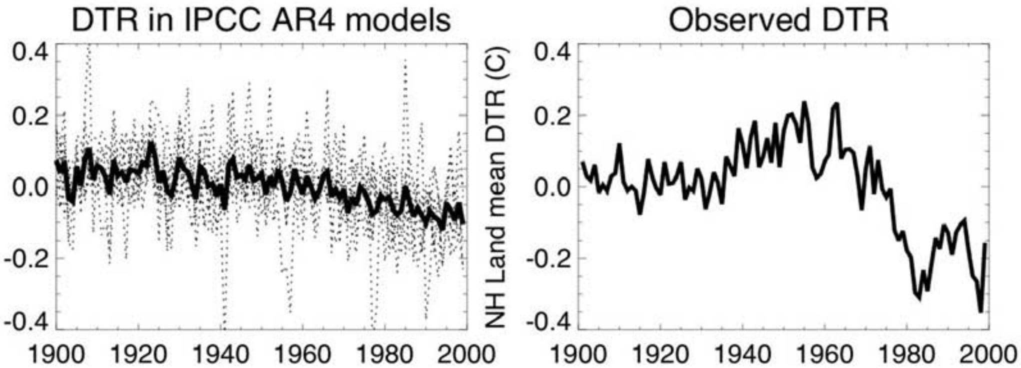

Figure 6. Annually averaged diurnal temperature range (DTR) anomalies over Northern Hemisphere land surfaces over the entire twentieth century, as (left) simulated by eight GCMs in twentieth-century experiments performed for the fourth IPCC assessment report and (right) observed. Multimodel mean is given as thick black line, and individual model realizations are shown as dashed lines. Observations from the CRU data set [*Mitchell and Jones*, 2005]. Reference period for anomalies is the entire twentieth century. Unit is °C.

[21] The lack of decadal variations in the models is even more evident when DTR simulations over terrestrial surfaces for the entire twentieth century are considered (Figure 6). I restrict myself to the terrestrial surfaces of the Northern Hemisphere, since only on the Northern Hemisphere there is abundant DTR information back to the early twentieth century for such an analysis (P. Jones, personal communication, 2008). The observed DTR evolution not only suggests a downward tendency predominantly between the 1950s and 1980s and a leveling off thereafter as discussed above, but also a slight upward tendency in the 1930s and 1940s (Figure 6, right). This provides indication for a brightening not only at the end of the twentieth century, but also in the 1930s and 1940s ("early brightening"), and suggests that the dimming was essentially confined to about a 30–40 years period in the second half of the twentieth century. A comparison with the DTR simulated in the models over the entire twentieth century (Figure 6, left) suggests that none of these decadal variations are reproduced by the models. Even though missing values in the observational data set are filled with climatologies if no other information is available (P. Jones, personal communication, 2008), which may dampen decadal variations in the observations, these variations are still much larger than simulated by the models. The "early brightening" indicated in the observed DTR record is in line with evidence from the few direct radiation measurements that reach back into the first half of the twentieth century, which show an increasing tendency in surface solar radiation during the 1930s and 1940s [*Ohmura*, 2006; *Wild*, 2009]. This is for example also seen in Figure 5 in the Stockholm time series. The lack of "early brightening" in the models may also explain their weaker than observed temperature rise in the early twentieth century.

[22] This lack in decadal variability in the GCM-calculated DTR and surface radiation fields could have various origins. An obvious origin could be an underestimated decadal variation in cloud characteristics, such as cloud cover and cloud albedo. Clouds were shown to have a major impact on DTR (through their modulation of the radiative fluxes) and can reduce the DTR by 25–50% compared with clear sky days over most land areas [*Dai et al.*, 1999]. Decadal variations of cloud characteristics are, however, not very well established from observations. Not even for the satellite era (since the early 1980s) we have unambiguous observational information on trends in these quantities. The strong decline in global mean cloud amount during the 1990s seen in the data of the International Satellite Cloud Climatology Project (ISCCP) [*Rossow and Duenas*, 2004] is controversial and currently disputed in the literature [e.g., *Evan et al.*, 2007]. Cloud estimates farther back in time have to rely on the historic synoptic observations based on human eye inspection of the sky, with associated uncertainties. An increased variation in cloud characteristics may be obtained in the models through the consideration of aerosol-cloud interactions (indirect aerosol effects). These effects are entirely neglected in most of the IPCC-AR4/CMIP3 models (see section 2 and *IPCC* [2007, Table 10.1]), or only crudely represented in a minority of these models. Inclusion of aerosol direct and indirect effects has a beneficial impact on the simulation of the DTR, as shown for example by *Quaas* [2003]. Also, the associated decadal variation in the distribution of atmospheric aerosol loads is not well known. Most IPCC-AR4/CMIP3 models prescribe the variations in sulfate (and some models additionally black carbon) burden in the atmosphere which may not contain the full extent of decadal variations, owing to a lack of better knowledge. *Ruckstuhl and Norris* [2009] find large discrepancies in different estimates on the evolution of sulfate and black carbon aerosol burdens over Europe which entered the IPCC-AR4 simulations, and consider this as a major cause for the inadequate simulation of the clear-sky surface solar radiation trends over Europe. Attempts are under way at several modeling centers to include the aerosol treatment more explicitly. These include the prescription of aerosol and aerosol precursor emissions based on emission inventories rather than prescribing atmospheric aerosol burdens, further include an explicit sulfur cycle, and consider interactive aerosol transport, transformation and deposition [e.g., *Stier et al.*, 2005]. This approach will allow for more flexibility and variability, once more accurate historic emission inventories are available with higher temporal resolution [e.g., *Bond et al.*, 2007]. Further, more sophisticated aerosol modules

now also include other interactive types of aerosol apart from sulfate, such as black and organic carbon, dust and sea salt. The emission-based approaches for various interactive aerosol types may increase the degrees of freedom of the global aerosol system, thereby increasing the variability, and in conjunction with direct and indirect aerosol effects may lead to larger variations in the radiative forcing. Of course it cannot be ruled out that besides the direct and indirect forcings, also other natural and anthropogenic forcings and their effects on clouds, radiation and DTR are underestimated in the models with respect to their decadal variations. For example, potential impacts of increasing greenhouse gases and associated warming on clouds are still poorly understood. Also, land surface feedbacks may be able to enhance or dampen decadal variability, although considered of secondary importance compared to the radiation and cloud effects in some studies [*Dai et al.*, 1999]. *Stone and Weaver* [2003] identified soil moisture changes, through their capability to change the ground heat capacity, as most important land surface feedback on DTR. Surface solar dimming was shown to be able to increase soil moisture by reducing the available energy for surface evaporation [*Robock et al.*, 2005]. Thereby, the DTR reduction caused by dimming could have been further pronounced by the increased soil moisture and associated increased heat capacity of the ground, and accordingly, the increasing DTR under brightening further enhanced through positive feedbacks. Climate models were shown to have difficulties in reproducing the observed decadal changes in soil moisture [*Robock et al.*, 2005].

[23] One should also keep in mind that we cannot exclude the possibility that the unforced natural variability of the climate system may not be reproduced by the models to its full extent. Such natural variability, for example, in the atmospheric dynamics, could potentially also induce decadal-scale variations in cloud properties independent of aerosol interactions, with associated surface solar radiation and DTR changes.

[24] Clearly, further work is required to elucidate the substantial discrepancies in the model-calculated and observed decadal variations in mean, daily maximum and minimum surface temperature as well as surface solar radiation identified in this study.

[25] **Acknowledgments.** This study is supported by the National Centre for Competence in Climate Research (NCCR Climate) of the Swiss National Science Foundation. I would like to express my gratitude to Christoph Schär for his continuous support of my work. I acknowledge the international modeling groups for providing their data for analysis, the Program for Climate Model Diagnosis and Intercomparison (PCMDI) for collecting and archiving the model data, the JSC/CLIVAR Working Group on Coupled Modeling (WGCM) and their Coupled Model Intercomparison Project (CMIP) and Climate Simulation Panel for organizing the model data analysis activity, and the IPCC WG1 TSU for technical support. The IPCC Data Archive at Lawrence Livermore National Laboratory is supported by the Office of Science, U.S. Department of Energy. Knut Makowski, Doris Folini, and Maria Hakuba, as well as two anonymous reviewers, are highly acknowledged for proofreading and helpful comments.

References

Alpert, P., P. Kishcha, Y. J. Kaufman, and R. Schwarzbard (2005), Global dimming or local dimming?: Effect of urbanization on sunlight availability, *Geophys. Res. Lett.*, *32*, L17802, doi:10.1029/2005GL023320.

Bond, T. C., E. Bhardwaj, R. Dong, R. Jogani, S. Jung, C. Roden, D. G. Streets, and N. M. Trautmann (2007), Historical emissions of black and organic carbon aerosol from energy-related combustion, 1850–2000, *Global Biogeochem. Cycles*, *21*, GB2018, doi:10.1029/2006GB002840.

Bristow, K. L., and S. Campbell (1984), On the relationship between incoming solar radiation and daily maximum and minimum temperature, *Agric. For. Meteorol.*, *31*, 159–166, doi:10.1016/0168-1923(84)90017-0.

Brohan, P., J. J. Kennedy, I. Harris, S. F. B. Tett, and P. D. Jones (2006), Uncertainty estimates in regional and global observed temperature changes: A new dataset from 1850, *J. Geophys. Res.*, *111*, D12106, doi:10.1029/2005JD006548.

Dai, A., K. E. Trenberth, and T. R. Karl (1999), Effects of clouds, soil moisture, precipitation, and water vapor on diurnal temperature range, *J. Clim.*, *12*, 2451–2473, doi:10.1175/1520-0442(1999)012<2451:EOCSMP>2.0.CO;2.

Easterling, D. R., et al. (1997), Maximum and minimum temperature trends for the globe, *Science*, *277*, 364–367, doi:10.1126/science.277.5324.364.

Evan, A. T., A. K. Heidinger, and D. J. Vimont (2007), Arguments against a physical long-term trend in global ISCCP cloud amounts, *Geophys. Res. Lett.*, *34*, L04701, doi:10.1029/2006GL028083.

Gilgen, H., M. Wild, and A. Ohmura (1998), Means and trends of shortwave irradiance at the surface estimated from Global Energy Balance Archive Data, *J. Clim.*, *11*, 2042–2061.

Hatzianastassiou, N., et al. (2005), Global distribution of Earth's surface shortwave radiation budget, *Atmos. Chem. Phys.*, *5*, 2847–2867.

Intergovernmental Panel on Climate Change (2007), *Climate Change 2007: The Physical Science Basis. Contribution of Working Group I to the Fourth Assessment Report of the Intergovernmental Panel on Climate Change*, edited by S. Solomon et al., Cambridge Univ. Press, Cambridge, U. K.

Karl, T. R., et al. (1993), Asymmetric trends of daily maximum and minimum temperature, *Bull. Am. Meteorol. Soc.*, *74*, 1007–1023, doi:10.1175/1520-0477(1993)074<1007:ANPORG>2.0.CO;2.

Kukla, G., J. Gavin, M. Schlesinger, and T. Karl (1995), Comparison of observed seasonal temperature maxima, minima and diurnal range in North America with simulations from three global climate models, *Atmos. Res.*, *37*, 267–275, doi:10.1016/0169-8095(94)00082-O.

Liepert, B. G. (2002), Observed reductions of surface solar radiation at sites in the United States and worldwide from 1961 to 1990, *Geophys. Res. Lett.*, *29*(10), 1421, doi:10.1029/2002GL014910.

Liu, B., M. Xu, M. Henderson, Y. Qi, and Y. Li (2004), Taking China's temperature: Daily range, warming trends, and regional variations, 1955–2000, *J. Clim.*, *17*, 4453–4462, doi:10.1175/3230.1.

Makowski, K., M. Wild, and A. Ohmura (2008), Diurnal temperature range over Europe between 1950 and 2005, *Atmos. Chem. Phys.*, *8*, 6483–6498.

Makowski, K., E. Jäger, M. Chiacchio, M. Wild, E. Tracy, and A. Ohmura (2009), On the relationship between diurnal temperature range and surface solar radiation in Europe, *J. Geophys. Res.*, *114*, D00D07, doi:10.1029/2008JD011104.

Mishchenko, M. I., I. V. Geogdzhayev, W. B. Rossow, B. Cairns, B. E. Carlson, A. A. Lacis, L. Liu, and L. D. Travis (2007), Long-term satellite record reveals likely recent aerosol trend, *Science*, *315*, 1543, doi:10.1126/science.1136709.

Mitchell, T. D., and P. D. Jones (2005), An improved method of constructing a database of monthly climate observations and associated high-resolution grids, *Int. J. Climatol.*, *25*, 693–712, doi:10.1002/joc.1181.

Norris, J. R., and M. Wild (2007), Trends in aerosol radiative effects over Europe inferred from observed cloud cover, solar "dimming," and solar "brightening," *J. Geophys. Res.*, *112*, D08214, doi:10.1029/2006JD007794.

Ohmura, A. (2006), Observed long term variations of solar irradiances at the Earth's surface, *Space Sci. Rev.*, *125*, 111–128, doi:10.1007/s11214-006-9050-9.

Pinker, R. T., B. Zhan, and E. G. Dutton (2005), Can satellites observe trends in surface solar radiation?, *Science*, *308*, 850–854, doi:10.1126/science.1103159.

Quaas, J. (2003), The aerosol indirect effect: Parameterization in large-scale models and evaluation with satellite data, doctoral thesis, 157 pp., Ecole Polytech., Lab. de Météorol. Dyn., Inst. Pierre Simon Laplace, Paris.

Robock, A., M. Mu, K. Vinnikov, I. V. Trofimova, and T. I. Adamenko (2005), Forty-five years of observed soil moisture in the Ukraine: No summer desiccation (yet), *Geophys. Res. Lett.*, *32*, L03401, doi:10.1029/2004GL021914.

Romanou, A., B. Liepert, G. A. Schmidt, W. B. Rossow, R. A. Ruedy, and Y. Zhang (2007), 20th century changes in surface solar irradiance in simulations and observations, *Geophys. Res. Lett.*, *34*, L05713, doi:10.1029/2006GL028356.

Rossow, W. B., and E. N. Duenas (2004), The International Satellite Cloud Climatology Project (ISCCP) web site: An online resource for research, *Bull. Am. Meteorol. Soc.*, *85*, 167–172, doi:10.1175/BAMS-85-2-167.

Ruckstuhl, C., and J. Norris (2009), How do aerosol histories affect solar "dimming" and "brightening" over Europe?: IPCC-AR4 models versus observations, *J. Geophys. Res.*, *114*, D00D04, doi:10.1029/2008JD011066.

Ruckstuhl, C., et al. (2008), Aerosol and cloud effects on solar brightening and the recent rapid warming, *Geophys. Res. Lett.*, *35*, L12708, doi:10.1029/2008GL034228.
Stanhill, G., and S. Cohen (2001), Global dimming: A review of the evidence for a widespread and significant reduction in global radiation with discussion of its probable causes and possible agricultural consequences, *Agric. For. Meteorol.*, *107*, 255–278, doi:10.1016/S0168-1923(00)00241-0.
Stern, D. I. (2006), Reversal of the trend in global anthropogenic sulfur emissions, *Global Environ. Change*, *16*, 207–220, doi:10.1016/j.gloenvcha.2006.01.001.
Stier, P., et al. (2005), The aerosol-climate model ECHAM5-HAM, *Atmos. Chem. Phys.*, *5*, 1125–1156.
Stone, D. A., and A. J. Weaver (2002), Daily maximum and minimum temperature trends in a climate model, *Geophys. Res. Lett.*, *29*(9), 1356, doi:10.1029/2001GL014556.
Stone, D. A., and A. J. Weaver (2003), Factors contributing to diurnal temperature range trends in twentieth and twenty-first century simulations of the CCCma coupled model, *Clim. Dyn.*, *20*, 435–445.
Streets, D. G., Y. Wu, and M. Chin (2006), Two-decadal aerosol trends as a likely explanation of the global dimming/brightening transition, *Geophys. Res. Lett.*, *33*, L15806, doi:10.1029/2006GL026471.
Vose, R. S., D. R. Easterling, and B. Gleason (2004), Maximum and minimum temperature trends for the globe: An update through 2004, *Geophys. Res. Lett.*, *32*, L23822, doi:10.1029/2005GL024379.
Wild, M. (2008), Shortwave and longwave surface radiation budgets in GCMs: A review based on the IPCC-AR4/CMIP3 models, *Tellus, Ser. A*, *60*, 932–945, doi:10.1111/j.1600-0870.2008.00342.x.
Wild, M. (2009), Global dimming and brightening: A review, *J. Geophys. Res.*, doi:10.1029/2008JD011470, in press.
Wild, M., A. Ohmura, H. Gilgen, and D. Rosenfeld (2004), On the consistency of trends in radiation and temperature records and implications for the global hydrological cycle, *Geophys. Res. Lett.*, *31*, L11201, doi:10.1029/2003GL019188.
Wild, M., et al. (2005), From dimming to brightening: Decadal changes in surface solar radiation, *Science*, *308*, 847–850, doi:10.1126/science.1103215.
Wild, M., C. N. Long, and A. Ohmura (2006), Evaluation of clear-sky solar fluxes in GCMs participating in AMIP and IPCC-AR4 from a surface perspective, *J. Geophys. Res.*, *111*, D01104, doi:10.1029/2005JD006118.
Wild, M., A. Ohmura, and K. Makowski (2007), Impact of global dimming and brightening on global warming, *Geophys. Res. Lett.*, *34*, L04702, doi:10.1029/2006GL028031.
Wild, M., J. Grieser, and C. Schär (2008), Combined surface solar brightening and increasing greenhouse effect support recent intensification of the global land-based hydrological cycle, *Geophys. Res. Lett.*, *35*, L17706, doi:10.1029/2008GL034842.

M. Wild, Institute for Atmospheric and Climate Science, ETH Zurich, Universitätstrasse 16, CH-8092 Zurich, Switzerland. (martin.wild@env.ethz.ch)